

HNBK-MR-BILSTM HYBRID MACHINE LEARNING MODEL FOR ENHANCED DIABETIC RETINOPATHY DETECTION IN FUNDUS IMAGING

ALKA SINGH¹, RAKESH KUMAR², AMIR H GANDOMI³

¹ Research Scholar, Department of Computer Science and Engineering, Madan Mohan Malaviya University of Technology, Gorakhpur, India

² Professor & Head of the Department, Computer Science and Engineering, Madan Mohan Malaviya University of Technology, Gorakhpur, India

³ Professor, Faculty of Engineering & Information Technology, University of Technology Sydney, Sydney, NSW, Australia

Email: ¹ alkaa.singh523@gmail.com, ² rkiitr@gmail.com, ³ a.h.gandomi@gmail.com

ABSTRACT

Utilizing a Computer-Aided Diagnosis (CAD) system of retinal fundus images is becoming optimal for manual fundus inspection. In addition, CAD of retinal fundus images was found to be more reliable and necessitated less time for both processing and analysis. Although several preprocessing techniques have been proposed, preprocessing remains challenging owing to a high level of contrast in the retinal vasculature network and image quality. In this work, a method called Hessian Niblack's Binarization Keypoint and Multi-scale Retinex Bidirectional LSTM (HNBK-MR-BiLSTM) for Diabetic Retinopathy detection is proposed. The HNBK-MR-BiLSTM is split into three sections: preprocessing, feature extraction, and classification for diabetic retinopathy detection. Based on the notion that the vessel profile could be modeled by separating into three channels, red, green and blue, the Hessian Frangi filter tries to model and preprocess the input images by retaining only the green channel while eliminating the red and blue channels for better representation of different types in fundus images via Second-order Partial Derivatives. Second, ophthalmoscopy was removed and combined the features from retina images based on Niblack's Threshold by binarization, as well as the coefficients of the rectangular array of pixels via PixMap. Finally, Bidirectional Multi-scale Retinex LSTM is applied to the keypoints detected for accurate classification between five distinct classes of images. Experimental results show that the proposed HNBK-MR-BiLSTM method for diabetic retinopathy learns more features of small targets and can efficiently enhance the classification performance of diabetic retina. The performance analysis of the proposed method to achieve better accuracy, time, sensitivity, specificity, and Peak Signal Noise Ratio (PSNR) compared to conventional methods is described. The results show that the proposed HNBK-MR-BiLSTM method improves at diagnosing diabetic retinopathy than more existing methods.

Keywords: *Diabetic Retinopathy, Hessian Frangi, Second-order Partial Derivatives, Niblack's Binarization, Keypoint, Nonlinear Feature Extraction, Multi-scale Retinex, BiLSTM*

1. INTRODUCTION

Diabetic Retinopathy (DR) ranks among the most widespread eye diseases, leading to vision impairment and can result in irreversible blindness if not treated. As the global population ages and diabetes cases continue to rise, DR has become a significant public health issue. Early detection is vital; however, the rising demand for ophthalmic evaluations is placing a burden on already limited clinical resources. Fundus photography is a standard technique for screening DR; nonetheless, accurate diagnosis is often obstructed by inconsistent lighting, varying color distributions, and deterioration of image quality. These issues complicate the detection of pathological features

such as microaneurysms, haemorrhages, and exudates, which are crucial indicators of disease severity. Ongoing monitoring after diagnosis is crucial for tracking disease progression and adjusting treatment plans. As a result, it is crucial to develop an automated and robust system for detecting DR to assist ophthalmologists, reduce diagnostic delays, and facilitate large-scale screenings. A variety of computer-aided diagnosis (CAD) systems, utilizing classical image processing and, more recently, deep learning approaches, have been suggested to tackle this problem. These systems are designed to improve diagnostic accuracy, minimize subjectivity, and promote early

intervention, ultimately aiding in the prevention of vision loss in diabetic patients.

In [1], RetNet-10 addressed a multiple-class classification issue for DR with a higher accuracy rate. Here, a shallow CNN was presented to address the time complexity and training time. Additionally, to address issues arising due to an imbalanced nature, data augmentation mechanisms were employed. Finally, to improve classification accuracy, the best configurations were determined, which prevented overfitting and underfitting during DR, resulting in high classification accuracy. However, the essential features of fundus images, such as the pathological pattern complexity, including shallow contrast in the image and distinct lesion magnitudes, affect the computer-aided design system's performance. In [2], the attention-based dual-path and multi-scale feature fusion network [ADP-MFFN] was designed with its feature. Here, we concentrated on minimal lesion features and obsessive distribution aspects by employing a dual-path attention mechanism. Additionally, a multi-scale feature fusion mechanism was designed that can fully utilise and combine distinct degrees of semantic information while discarding insignificant information, thereby significantly improving precision, accuracy, and recall rate. Five stages of DR were detected in [3] employing a multitask deep learning model [MDLM]. Here, an enhanced deep neural network model employing the Squeeze Excitation Dense function was designed as a part of the multitasking approach. For real-time applications, the detection of diabetic retinopathy using automated mechanisms is necessary to both assist and minimize potential human errors.

In [4], a feature selection method combining a deep neural network and the genetic algorithm was presented. These fusion methods resulted in an improvement in accuracy. To authorise a person's eye, several visualisation methods have been designed and developed over the past few years. Retinal imaging has gained a reputation among them due to its non-invasive and cost-efficient factors. Different types of ocular structures and biomarkers, which exhibit various abnormalities, can be identified. Additionally, numerous techniques play a significant role in the identification of retinal diseases. In [5], a neural network was designed with a continuous and densely connected structure via adaptive rate dropout for the classification of DR. This design enabled accurate and timely classification at three distinct levels. However, another validation method was designed in [6] using

a deep learning system. An elaborate review of deep learning techniques for DR was conducted in [7].

One of the microvascular diseases arising due to diabetes is DR, and it is held to be the leading cause of blindness and image destruction globally. In addition to different numbers, DR is said to be split into five classes. Hence, it is said to be significant in grading DR severity; therefore, patients suffering from DR can receive treatment both accurately and promptly. An attention mechanism was designed in [8], consisting of a category attention block and a global attention block, which not only obtained discriminative features but also obtained features globally. However, another attention mechanism employing a new feature map for fine-tuning via cosine annealing learning rate was presented in [9]. With this attention, the mechanism resulted in the improvement of accuracy with high sensitivity and specificity.

Even though a large number of deep learning-based diabetic retinopathy-detection models have been suggested, current solutions still have shortcomings related to poor-image quality sensitivity, fine vascular-structure preservation, micro-lesion amplification, computational and memory efficiency, as well as multi-class classification reliability across different datasets. These unsolved problems inspire the creation of a more powerful, explainable, and calculable hybrid framework to detect accurate DR. The suggested framework provides good hybrid modelling, high micro-lesion preservation, high clinical reliability, low computational cost, and good statistical validation. These limitations consist of one-dataset testing, no external testing, manual tuning, and no clinical trials. Future directions will be related to multi-dataset validation, integration of transformers, explainable AI, mobile deployment, and clinical research.

In the context of the above work, a novel method known as the Hessian Niblack's Binarization Keypoint and Multi-scale Retinex Bidirectional LSTM (HNBK-MR-BiLSTM) for Diabetic Retinopathy detection is proposed for retinal images. Initially, it was preprocessed to fundus images by using the diabetic retinopathy arranged dataset. This process is utilized in turning images into noise-minimized, enhanced contrast images. Adopting the Hessian Frangi filter via Second-order Partial Derivatives uninterruptedly enhances the fundus retinal images' performance. Then, the processed retinal images are subjected to extraction and classification based on the Bidirectional Multi-scale Retinex LSTM. Then, features are extracted, and the extracted features are confidential by obtaining an

optimized activation function. Subsequently, the metrics are fine-tuned using the Hessian Frangi filter. Finally, this method enhanced classification accuracy, correctly classifying descriptions as normal, mild, moderate, severe, and proliferative.

1.1 Key Contributions

- A new method called Hessian Niblack's Binarization Keypoint and Multi-scale Retinex Bidirectional LSTM (HNBK-MR-BiLSTM) for DR detection.
- A novel vessel preprocessing model using the Hessian Frangi Second-order Partial Derivatives-based Preprocessing algorithm that needs less processing time and allows us to obtain different types of fundus image lesions, improving the peak signal-to-noise ratio.
- A novel Niblack's Binarization Keypoint Nonlinear Feature Extraction algorithm was performed to extract precise and accurate keypoints via the Binarization Keypoint Nonlinear factor.
- A novel Bidirectional Multi-scale Retinex LSTM for diabetic retinopathy detection that, with the aid of single-scale and multi-scale retinex function, correctly classifies the processed color retina images, then the sensitivity and specificity rate was improved.
- The novelty has now been explained by clearly pointing out the fact that the proposed HNBK-MR-BiLSTM is the first to combine Hessian-Frangi vessel enhancement, Niblack keypoint extraction, Multi-scale Retinex illumination correction, and BiLSTM sequential learning.
- Extensive experimental verification is more accurate, sensitive, and specific, with high PSNR and lower inference time than state-of-the-art.

Performance analysis of the proposed HNBK-MR-BiLSTM method compared with existing methods, RetNet-10 [1], and attention-based dual-path and multi-scale feature fusion network [2] in the diagnosis of DR, has been drawn to validate our method and findings.

1.2 Organization of the Paper

The paper is organised into different sections, followed by Section 2, which presents a literature survey on reviews related to DR diagnosis. In

Section 3, the proposed Hessian Niblack's Binarization Keypoint and Multi-scale Retinex Bidirectional LSTM (HNBK-MR-BiLSTM) for Diabetic Retinopathy detection is elaborated with the aid of algorithmic representation. The experimental analysis of the proposed HNBK-MR-BiLSTM Method and existing methods is designed in Section 4. At last, to conclude the discussion depicted in Section 5.

2. LITERATURE REVIEW

Regarding the healthcare domain, disease treatment is said to be more efficient when detected at an early stage. The lack of sufficient insulin results in an increase in glucose levels, leading to diabetes. Some of the parts said to be affected by diabetes are the retina, nerves, kidneys, and heart. The occurrence of DR is owing to the complexity of diabetes, as well as the swelling of blood vessels, which causes fluid leakage. Several research works have contributed to DR recognition. In [10], a review of deep learning techniques in the domain of DR recognition was introduced. Over the past few decades, the growth of AI techniques, specifically DL-based algorithms, has been extensively utilized for detecting DR. With this objective, DR diagnosis from retinal images using DL was utilized by the domain investigated in [11]. The significant DR diagnosis and detection method is said to be both laborious and time-consuming, owing to the lack of both resources and expert opinion. Due to this, computer-aided diagnosis mechanisms using DL have received significant attention in the research community.

In [12], a holistic mechanism employing twenty-six different types of DL networks for both assessing and validating their performance was investigated. The eye diseases of DR are rapidly developing and have increased over the past few years. The complicated nature of diabetes results in blood vessel damage and subsequently results in vision loss and, in certain cases, even blindness. In the contemporary world, elevated blood pressure and blood sugar are the basic keys that decline in older people. Hence, early detection of DR is mandatory for significant improvement.

A novel automatic detection of severity employing a single color fundus image via deep learning was presented in [13]. Also, the block attention module was employed to minimize both the time and complexity factors involved in DR classification. Nevertheless, most of the prevailing methods necessitate several DR annotations for efficient training. Also, the fundus images acquired differ to

distinct degrees according to the shooting tools in use. As a result, results in inefficient detection. To focus on this feature, GATL for DR diagnosis was performed in [14] to transfer learning, intra-domain alignment, and inter-domain alignment. With this alignment mechanism, the sensitivity and specificity rates were said to be improved extensively. Screening for DR necessitates ophthalmologists to measure retinal images, and it has developed into a more laborious and unwieldy process in providing expert eye care to all, owing to the rapid increase in the diabetes population. Nevertheless, DR screening has to be performed on a routine basis, which places a great amount of sensitivity on accomplished owing to the growing number of diabetic patients, resulting in delays.

The elevated research gap has resulted in the requirement for DR screening in an automated manner. Visualization was applied to enhance the module calibration and predict DR in an accurate fashion [15]. As a result, the overfitting issue was addressed, therefore improving the accuracy in a significant manner. A review of DR identification using deep learning techniques was investigated in [16]. Nevertheless, these mechanisms are found to be both computationally elevated in terms of expense and also lack in extracting nonlinear features and, henceforth, fail in classifying different classes. The lowest possible learnable parameters were employed in [17] to speed up the training process with high convergence. A mechanism for classifying retinal fundus images was designed in [18] based on the integration of multi-scale shallow CNNs. A survey of deep learning techniques employing fundus images for detecting eye disease was investigated in [19]. Yet another review of DR detection and classification techniques employing

Nonetheless, challenges such as dependence on adequate labeled data, the risk of model overfitting with small datasets, and the requirement for computational efficiency for real-time use still need further investigation. Table 1 gives a summary of the related work. We have clearly specified the research

deep learning was presented in [20]. In [21], a novel method for DR diagnosis based on fundus images using a decision tree-based ensemble learning technique is designed.

Although there has been notable advancement in the detection of diabetic retinopathy (DR) through machine learning and deep learning approaches, several challenges remain that influence diagnostic precision and generalizability. Typical constraints include subpar image quality due to variable lighting, insufficient enhancement of small lesions, inadequate lesion localization, and a limited ability to classify multiple categories. Additionally, numerous current models approach DR detection as a binary issue, lack interpretability, and do not perform well when confronted with the intricate structural variations found in retinal images. To tackle these challenges, the suggested HNBK-MR-BiLSTM approach combines a structured process involving preprocessing, feature extraction, and classification. By applying the Hessian Frangi filter to the green channel, vessel visibility is enhanced while the effects of color and lighting inconsistencies are reduced. The use of Niblack's thresholding and PixMap encoding allows for localized binarization and the isolation of structural features, which helps in identifying small pathological patterns. Moreover, incorporating a Bidirectional Multi-scale Retinex LSTM network enables the model to understand contextual relationships across various retinal regions, leading to accurate classification across five different stages of DR. This all-encompassing framework effectively addresses issues related to image quality, representation of lesion features, and classification depth, thus enhancing both the interpretability and diagnostic accuracy of the system.

gap of preservation of micro-lesions, robustness of illumination, computational efficiency, and dependable multi-grade DR classification. A new table and discussion on the limitations of the previous work versus the input of our study have been introduced.

Table 1: Summary table for the related works

Authors	Proposed Methodology	Dataset Used	Sensitivity	Specificity	Accuracy
Silvia Rego et al. [22]	Inception-V3 with CNN model	EyePACS	80.8%	95.6%	-
Sajib Kumar Saha et al. [23]	Deep convolutional neural-network	EyePACS	100%	100%	100%
Qaisar Abbas et al. [24]	Gradient location orientation histogram (GLOH), DColor-SIFT and deep learning neural-network	DIARETDB 1, MESSIDOR & Custom dataset	92.18%	94.50%	-
Huazhu Fu et al. [25]	Fully connected conditional random field (FCCRF) and FCN	DRIVE and STARE	71.40%	-	95.45%
Juan Mo and Lei Zhang [26]	Multi-level hierarchical fully convolutional network (FCN) approach	DRIVE, STARE, and CHASE_DB 1	81.47%	98.44%	98.85%
Debapriya Maji et al. [27]	Deep neural-network (DNN) and stacked ne-noising auto-encoder	DRIVE	-	-	93.27%
K. V. Maya et al. [28]	Recursive region growing segmentation (RRGS), Laplacian Gaussian Filter (LGF), CNN	MESSIDOR	96.99%	96.51%	98.25%
C. Rajaa et al. [29]	Adaptive histogram equalization (AHE) plus fuzzy c-means clustering (FCM), CNN	Diabetic retinopathy database	98.1%	99%	93.2%
Tang F et al. [30]	ResNet-50 and transfer learning approach	Custom dataset	86.5%	82.1%	-
Cam-Hao Hua et al. [31]	Skip-connection deep networks (Tri-SDN) architecture	Custom dataset	96.5%	82.1%	90.6%
Sehrish Qummar et al. [32]	Inception-V3, Resnet50, Dense-121, Dense-169, and Xception	Kaggle	-	86.7%	80.8%
Ambaji S. Jadhav et al. [33]	Modified gear and steering- Rider optimization algorithm (MGS-ROA) and deep belief network-based model	DIARETDB 1	86.36%	95.45%	93.18%

Authors	Proposed Methodology	Dataset Used	Sensitivity	Specificity	Accuracy
D. Jude Hemanth et al. [34]	Histogram equalization, CLAHE, CNN	MESSIDOR	94%	98%	97%
Ramzi Adriman et al. [35]	Local binary patterns (LBP), ResNet	APTOS 2019 Blindness	-	-	96.36%
Emmy Bhatti and Prabhpreet Kaur [36]	Gaussian filter (GF) and multi-support vector machine (MSVM)	DIARETDB 0	82.66%	82%	82%

3. PROPOSED METHODOLOGY

Usual exposure to DR gives an early mechanism utilized to craft a certain therapy via a specialist surgeon. Hence, it is essential to work on quality in analysis with treatment. To automate and identify the diabetic retinopathy process, different deep learning-based examined in the proposed work in the literature in an end-to-end manner. In the previous section, these methods involve the addition of an

attention apparatus to extract highly nonlinear features and patterns inside the fundus images to determine the specific class of diabetes from the image itself. Figure 1 illustrates the methodology of a computer-aided diabetic retinopathy diagnosis system called Hessian Niblack’s Binarization Keypoint and Multi-scale Retinex Bidirectional LSTM (HNBK-MR-BiLSTM) for Diabetic Retinopathy detection.

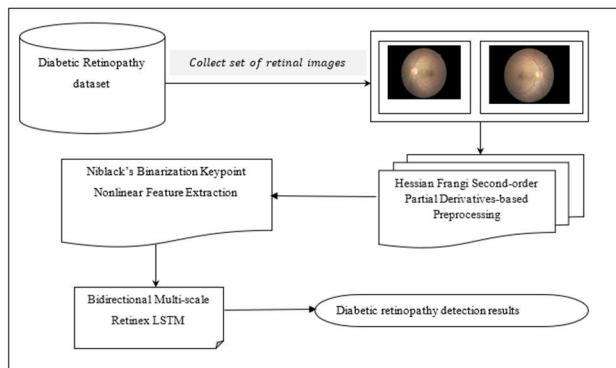


Figure 1: Structure of Hessian Niblack’s Binarization Keypoint and Multi-scale Retinex Bidirectional LSTM (HNBK-MR-BiLSTM) for Diabetic Retinopathy detection

Figure 1 represents the benchmark diabetic retinopathy arranged dataset [37] of five different classes (i.e., No DR, Mild, Moderate, Severe, Proliferative DR) is loaded into the system, combined into each distinct sub-dataset, i.e., training set and verified data. In splitting the dataset, a holdout cross-validation method is employed that partitions the given raw dataset with a percentage of 70:30, where ‘70%’ of images from five different classes are selected in an arbitrary fashion for model training along with their labels, while the remaining ‘30%’ images with their corresponding labels are

chosen as a validation set that is used in evaluating the proposed method’s performance. The sample retinal images are split into red, green, and blue channels using the preprocessing stage. Red, blue, and green channels consist of further delegated information with improved differentiation between lesion types in fundus images. As a result, the green channel is selected by employing Hessian Frangi Second-order Partial Derivatives-based Preprocessing. In the feature extraction module, Niblack’s threshold and Binarization Keypoint Nonlinear factors are chosen to correspondingly remove the lesion’s keypoints. In the classification stage, the Bidirectional Multi-scale Retinex LSTM is used to classify targets. In the next subsections, each part will be discussed in more detail.

3.1 Hessian Frangi Second-order Partial Derivatives-based Preprocessing

The initial step in DR recognition is to assess the optic disc. The fundus image is an RGB color image that involves three channels (i.e., red, green, and blue). To aspect visual disc, diabetic retinopathy identification is achieved by splitting the fundus of the image into three channels. The vessels in the fundus image are visible in the red channel, except that this channel comprises saturated noise, whereas the blue channel is distinguished by minimum contrast and fails to include much information. At last, the green channel provides the best result, and then the green image channel is applied in automatic

retinal image analysis. Hence, this work selects the green channel as input by employing the Hessian Frangi Second-order Partial Derivatives-based Preprocessing model.

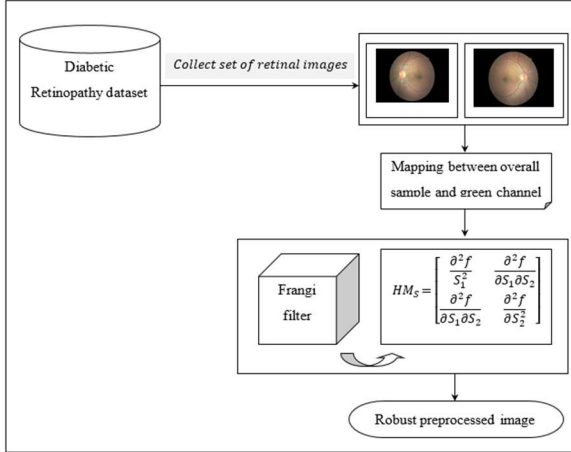


Figure 2: Structure of Hessian Frangi Second-order Partial Derivatives-based Preprocessing

As illustrated in the above figure, a set of retinal images is acquired from the diabetic retinopathy dataset. With five different types of specific class labels performed in the dataset, the aim here remains to identify DR in a computationally efficient and precise manner. The above sample retinal images show left and right no-DR retinal images obtained from the diabetic retinopathy dataset. To start with, the input retina images acquired from the Diabetic Retinopathy dataset, an input vector is formulated as given below.

$$IV \rightarrow \{S_1SS_1, S_2SS_1, \dots, S_mSS_n\} \quad (1)$$

In the formulation (1), the input vector ‘IV’ is modeled by taking into consideration ‘S_m’ sample retinal images involved in simulation process and retinal sample size ‘SS_n’ respectively. The input fundus image from DR dataset possesses a distinct purpose (i.e., red, green and blue). With distinct resolutions in vogue, a mapping between the overall sample and green channel is performed as given below.

$$Res(G_k) = \sum_{k=1}^l PDF_G(G_k) \quad (2)$$

In Equation (2), ‘PDF_G’ denotes the probability density function of the green channel image and stored in the form of an intermediate resultant matrix ‘Res(G_k)’ respectively. As already mentioned, the

retinal image in RGB color space is separated into discrete channels, red, green, and blue, to calculate the difference between green channels and recognize the proliferation of distinct green channels. Data variability is mathematically represented as given below.

$$\sigma = \frac{1}{mn} \sum_{i=1}^m \sum_{j=1}^n [S(i, j) - \mu]^2 \quad (3)$$

In Equation (3), ‘S(i, j)’ is an individual pixel in Sample Retinal Images ‘S’, mean ‘μ’ and frequency of green channel rows and columns. A Frangi Filter is then applied to perform noise removal, as it requires less computation time. This Frangi Filter is applied to distinct green channels data variability via the Hessian Matrix by measuring the parallel and perpendicular Sample Retinal Images diagonals. This is mathematically represented as given below.

$$Fil(S[PoI]) = Max_{\sigma} Fil(S[PoI], \sigma) \quad (4)$$

In Equation (4), the pixel of interest for the corresponding sample retinal images is defined by ‘S[PoI]’, standard deviation denoted as ‘σ’ and ‘Fil’ representing the filter. The Hessian Matrix is then mathematically stated as given below.

$$HM = \begin{bmatrix} HM_{xx}[Fil(S[PoI])] & HM_{xy}[Fil(S[PoI])] \\ HM_{yx}[Fil(S[PoI])] & HM_{yy}[Fil(S[PoI])] \end{bmatrix} \quad (5)$$

In the formulation (5), ‘HM_{xx}’, ‘HM_{xy}’, ‘HM_{yx}’ and ‘HM_{yy}’ represents the Second-order Partial Derivatives for the corresponding parallel and perpendicular Sample Retinal Images diagonals, respectively. Finally, the Hessian Frangi filter is applied to preserve the edges between points of interest in the sample image and is mathematically formulated as given below.

$$PI = Fil(S[PoI]) = \begin{cases} 0, & \text{if } \gamma_2 > 0 \\ e^{\left(\frac{Res(G_k)}{2\gamma_1^2}\right)} \left(1 - e^{\left(\frac{Res(G_k)}{2\gamma_2^2}\right)}\right), & \text{Otherwise} \end{cases} \quad (6)$$

In the Equation (6) with the fine-tuned parameters ‘γ₁ = 0.01’ and ‘γ₂ = 0.02’, provides the best overall representation of distinct types of lesions in fundus images. The pseudo-code representation of

the Hessian Frangi Second-order Partial Derivatives-based Preprocessing is given below.

Algorithm 1: Hessian Frangi Second-order Partial Derivatives-based Preprocessing
Input: Dataset ‘ DS ’, Sample Retinal Images ‘ $S = \{S_1, S_2, \dots, S_m\}$ ’, Retinal Image Size ‘ $SS = \{SS_1, SS_2, \dots, SS_n\}$ ’
Output: Noise eliminated robust preprocessed image
1: Initialize ‘ $m = 35000$ ’, Retinal Image Size ‘ SS ’, ‘ $\gamma_1 = 0.01$ ’, ‘ $\gamma_1 = 0.02$ ’
2: Begin
3: For each Dataset ‘ DS ’ with Sample Retinal Images ‘ S ’ and Retinal Image Size ‘ SS ’
4: Formulate input vector matrix as given in (1)
5: Perform mapping between the overall sample and green channel as given in (2)
6: Measure the variance of the green channel as given in (3)
7: Estimate Frangi Filter via Hessian Matrix as given in (4) and (5)
8: Return preprocessed image as given in (6)
9: End for
10: End

In Algorithm 1, the input images are first subjected to the Frangi filter to increase both noise and computation time in DR identification. This filter is applied only to the green channel because the green channel comprises much more image information and assists in denoting different types of fundus image lesions. As a result, the computation time involved in the DR identification process gets removed. Next, the filtered resultant green images are subjected to Frangi Second-order Partial Derivative that, in turn, preserves the edges between points of interest in the sample image and, therefore, improves the noise ratio significantly.

3.2 Niblack’s Binarization Keypoint Nonlinear Feature Extraction Model

Feature extraction refers to the procedure of transforming raw data or image data into numerical features that are again processed to preserve the information in the original dataset. By performing efficient feature extraction is said to yield better results upon comparison with the direct classification of the raw data. On the other hand, the keypoint detector predicts a score vector that signifies each candidate’s perspective being a

keypoint. The feature extractor is optimized to learn robust keypoint features by utilizing the correspondence between keypoints generated from two inputs (i.e., training image and testing image). Using keypointdetector, nonlinear concentric points are said to be detected that stand out in retinal images. In our work, Niblack’s Binarization Keypoint Nonlinear Feature Extraction model is designed by extracting image keypoint, even in the image scale resolution changes and orientation. Figure 3 shows the structure of Niblack’s Binarization Keypoint Nonlinear Feature Extraction is given below.

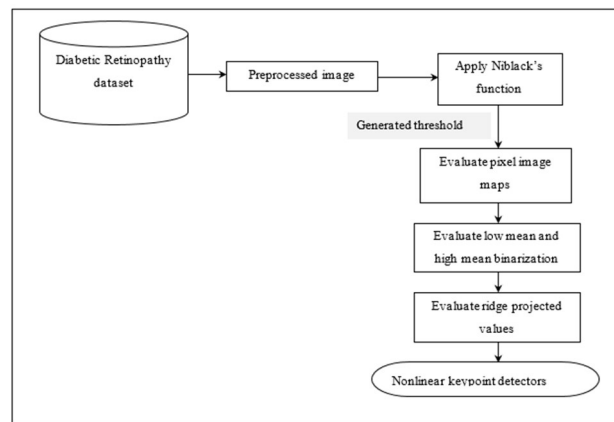


Figure 3: Structure of Niblack’s Binarization Keypoint Nonlinear Feature Extraction

As illustrated in Figure 3, with the objective of reducing the false positive and false negative cases while detecting diabetic retinopathy, keypoints should be detected in an accurate and precise manner. With this objective, the threshold to obtain the keypoints is initially modeled using Niblack’s function. Following this, pixel image maps are obtained subject to the threshold value. Next, low mean and high mean binarization on the green color component sample preprocessed retinal image are obtained and subjected to Binarization Keypoint Nonlinear factor to detect significant keypoints. Let us consider a preprocessed image ‘ PI ’ as input of size ‘ $m * n$ ’, then, the threshold for each pixel in the green color channel is obtained by employing Niblack’s function formulated as,

$$Th(PI) = \frac{1}{(m*n)} * \sum_{i=1}^m \sum_{j=1}^n PI(i,j) + Cons * \sigma \tag{7}$$

From the above Equation (7), the threshold for each preprocessed image ‘ $Th(PI)$ ’ is obtained by taking into consideration the constant ‘0.5’ with respect to

the green color channel. Following this, the pixel image maps for each preprocessed image 'PixMap_{PI}' with size '(i, j)' is obtained as given below.

$$PixMap_{PI}(i, j) = \begin{cases} 1, & \text{if } PI(i, j) > Th \\ 0, & \text{if } PI(i, j) < Th \end{cases} \quad (8)$$

With the obtained pixel image maps for each preprocessed image, image features for the green color component sample preprocessed retinal image are modeled subject to low and high mean that tracks the frequency of times two levels of intensity 'i' and 'j' occur at orientation 'θ'. This is mathematically represented as given below.

$$PI_{HMean} = \frac{1}{\sum_{i=1}^m \sum_{j=1}^n PixMap_{PI}(i, j)} * \sum_{i=1}^m \sum_{j=1}^n PixMap_{PI}(i, j) * PI(i, j) \quad (9)$$

$$PI_{LMean} = \frac{1}{m*n - \sum_{i=1}^m \sum_{j=1}^n PixMap_{PI}(i, j)} * \sum_{i=1}^m \sum_{j=1}^n (1 - PixMap_{PI}(i, j)) * PI(i, j) \quad (10)$$

In Equations (9) and (10), 'PI_{HMean}' refers to high mean and 'PI_{LMean}' denotes low mean binarization on the green color component of the sample preprocessed retinal image, respectively. Finally, to detect keypoints even in the resolution and orientation changes, the ridge projection for each preprocessed image is obtained as given below.

$$R(p, q, \theta) = \int \psi_{p,q,\theta}(PI) f(PI) dPI \quad (11)$$

$$\psi_{p,q,\theta}(PI) = p^{-1/2} \psi ([PI_1 \cos \theta + PI_2 \sin \theta - q] / p) \quad (12)$$

From the above Equations (11) and (12), the scaling factors in retinal preprocessed images and their orientation in space are obtained, therefore ensuring or detecting keypoints with minimum falsification. Finally, the keypoint detected results are obtained as given below.

$$KPD_{PI}(i, j) = \begin{cases} 1, & \text{if } PI(i, j) > PI_{HMean} \text{ And } PI(i, j) < PI_{LMean} \\ 0, & \text{if } PI(i, j) > PI_{LMean} \text{ And } PI(i, j) < PI_{HMean} \end{cases} \quad (13)$$

The pseudo-code representation of Niblack's Binarization Keypoint Nonlinear Feature Extraction is given below.

Algorithm 2: Niblack's Binarization Keypoint Nonlinear Feature Extraction

Input: Dataset 'DS', Sample Retinal Images 'S = {S₁, S₂, ..., S_m}', Retinal Image Size 'SS = {SS₁, SS₂, ..., SS_n}'

Output: precise and accurate keypoint detected (i.e., keypoint extracted)

- 1: **Initialize** 'm = 35000', Retinal Image Size 'SS', preprocessed image 'PI' [for each pixel in green color channel], constant 'Cons = 0.5'
- 2: **Begin**
- 3: **For** each Dataset 'DS' with Sample Retinal Images 'S', Retinal Image Size 'SS' and preprocessed image 'PI'
- 4: Determine the threshold as given in (7)
- 5: Evaluate pixel image maps for each preprocessed image as given in (8)
- 6: Evaluate high mean and low mean binarization on green color component sample preprocessed retinal image as given in (9) and (10)
- 7: Obtain the orientation results as given in (11) and (12)
- 8: **If** 'PI(i, j) > PI_{HMean} & And PI(i, j) < PI_{LMean}'
- 9: Keypoints are detected
- 10: Obtain the detected results
- 11: **Return** keypoints detected 'KPD'
- 12: **End if**
- 13: **If** 'PI(i, j) > PI_{LMean} And PI(i, j) < PI_{HMean}'
- 14: No keypoints are detected
- 15: **Go to** step 3
- 16: **End if**
- 17: **End for**
- 18: **End**

As given in Algorithm 2, Niblack's Binarization Keypoint Nonlinear Feature Extraction allows us to remove the determination of data standing for preprocessed images. In the hypothesis, which keypoints may occur due to dark vascular structure, while the optic disc is bright as in green color element, the keypoints associated with this region are identified so that the false positive and false negative cases can be reduced significantly. With this objective initially, Niblack's function is utilized for modeling the threshold. Second, with the pixel image maps as input, high mean and low mean binarization on the green color component is obtained. Third, the orientation factor was also taken into consideration to detect keypoints even in the shift in resolution and orientation. As a result, the sensitivity and specificity of efficient keypoints were detected.

3.3 Bidirectional Multi-scale Retinex LSTM-based Diabetic Retinopathy

Finally, classification is carried out by the Bidirectional Multi-scale Retinex LSTM gathering to correctly realize the classification of diabetic fundus images at different specific class labels (No DR, mild, moderate, severe, and proliferative DR), respectively. An illumination correction model is necessary in diabetic retinopathy detection due to the complex nature of retinal fundus images. In this work, the Multi-scale Retinex function is applied to the Bidirectional LSTM or BiLSTM to obtain the classified resultant output with a higher rate of accuracy. Figure 4 shows the Bidirectional Multi-scale Retinex LSTM structure for diabetic retinopathy detection.

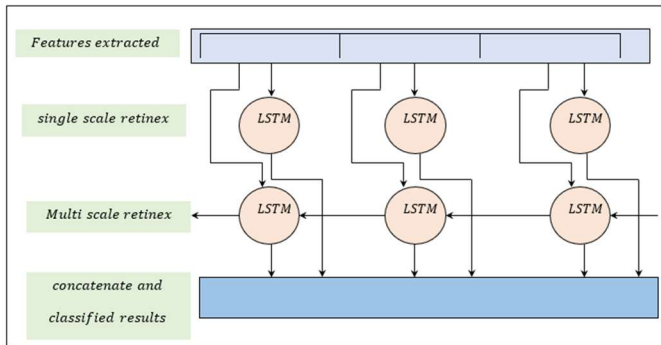


Figure 4: Structure of Bidirectional Multi-scale Retinex LSTM for diabetic retinopathy detection

In Figure 4, the BiLSTM consists of two LSTMs, one taking the preprocessed keypoints in the input direction, whereas the other takes the preprocessed keypoints in the reverse direction, knowing what pixels immediately follow and precede a pixel in a diabetic fundus image. In our work, the single-scale retinex function is applied in the input direction, whereas the scale retinex function is applied in the reverse direction. Let us consider the single-scale retinex function for the subsequent key point detected preprocessed image as given below.

$$R(i, j) = \log[PI(KPD(i, j))] - \log[f(i, j) * PI(KPD(i, j))] \quad (14)$$

From the above Equation (14), the single scale retinex resultant image 'R(i, j)' is arrived at by taking into consideration the point detected preprocessed input image 'PI(KPD(i, j))' Gaussian function 'f(i, j)', retinex output 'R(i, j)' with respect to convolution '*' respectively.

$$f(i, j) = U \cdot e^{(i^2+j^2)/C^2} \quad (15)$$

The Gaussian function 'f(i, j)' output as given above (15) is obtained based on the angular movement 'C' whereas the function 'U' is determined as given below.

$$U = \int f(i, j) didj = 1 \quad (16)$$

However, to restore the information owing to the presence of different intensities in different regions in the original picture, recombination is required to restore the information to ensure accurate and precise classification. This is performed by applying the multi-scale retinex function as given below.

$$R_{MSR_{i,j}} = \sum \log PI(KPD(i, j)) - \log[f(i, j)] * PI(KPD(i, j)) \quad (17)$$

Next, the concatenate function is evolved as given below.

$$ResOp = R(i, j) \cap R_{MSR_{i,j}} \quad (18)$$

Finally, the optimized activation function to obtain the classified results is mathematically stated as given below.

$$f(ResOp) = \max(g(ResOp), ResOp) \quad (19)$$

$$g(ResOp), ResOp = \frac{ResOp}{1+e^{-\gamma Res}} \quad (20)$$

Based on the above resultant values, accurate and precision diabetic retinopathy results are obtained. The pseudo-code representation of Bidirectional Multi-scale Retinex LSTM is given in Algorithm 3.

In Algorithm 3, to increase the accuracy and time consumed in the detection of diabetic retinopathy, the multi-scale retinex function is subjected to Bidirectional LSTM. Here, both the single-scale retinex function and the multi-scale retinex function are applied to the subsequent key points detected. Then, according to the sequence processing model, it efficiently improves the information available to the algorithm, producing significant classification results. Also, applying the optimized activation function results in precise and specific detection of diabetic retinopathy in a timely manner.

Algorithm 3: Bidirectional Multi-scale Retinex LSTM
Input: Dataset ‘ DS ’, Sample Retinal Images ‘ $S = \{S_1, S_2, \dots, S_m\}$ ’, Retinal Image Size ‘ $SS = \{SS_1, SS_2, \dots, SS_n\}$ ’
Output: Robust diabetic retinopathy detection
<p>1: Initialize ‘$m = 35000$’, Retinal Image Size ‘SS’, preprocessed image ‘PI’ [for each pixel in green color channel], keypoints detected ‘KPD’</p> <p>2: Begin</p> <p>3: For each Dataset ‘DS’ with Sample Retinal Images ‘S’, Retinal Image Size ‘SS’, preprocessed image ‘PI’ and keypoints detected ‘KPD’</p> <p>4: Evaluate single scale retinex function for the subsequent key point as given in (14), (15) and (16)</p> <p>5: Evaluate multi scale retinex function for the subsequent key point as given in (17)</p> <p>6: Concatenate single scale retinex function results with multi scale retinex function results as given in (18)</p> <p>7: Evaluate classified results as given in (19) and (20)</p> <p>8: If ‘$g(ResOp), ResOp = 0$’</p> <p>9: Then fundus image detected with No DR</p> <p>10: End if</p> <p>11: If ‘$g(ResOp), ResOp = 0 \text{ to } 0.25$’</p> <p>12: Then fundus image detected with mild DR</p> <p>13: End if</p> <p>14: If ‘$g(ResOp), ResOp = 0.25 \text{ to } 0.50$’</p> <p>15: Then fundus image detected with moderate DR</p> <p>16: End if</p> <p>17: If ‘$g(ResOp), ResOp = 0.50 \text{ to } 0.75$’</p> <p>18: Then fundus image detected with severe DR</p> <p>19: End if</p> <p>20: If ‘$g(ResOp), ResOp = 0.75 \text{ to } 1$’</p> <p>21: Then fundus image detected with proliferative DR</p> <p>22: End if</p> <p>23: End for</p> <p>24: End</p>

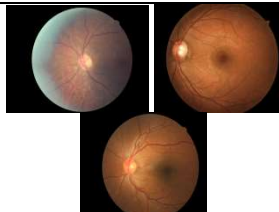
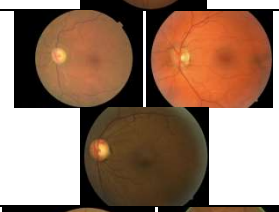
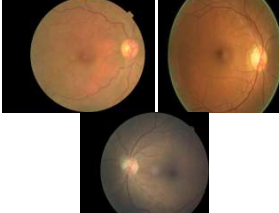
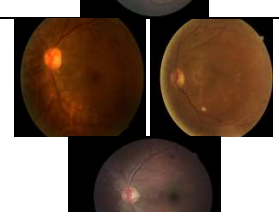
4. PERFORMANCE ANALYSIS

4.1 Dataset Description

To appraise the detection performance of the proposed HNBK-MR-BiLSTM method, this paper carried out the validation of the scheme in a public dataset named diabetic retinopathy arranged dataset taken from <https://www.kaggle.com/amanneo/diabetic-retinopathy-resized-arranged>. This dataset is

utilized to evaluate fundus images with class labels for classification. This dataset was utilized in evaluating the illustration of detection for DR. The dataset comprises digital images with five different specific class labels. The distribution of samples in 5 different classes namely are, No DR, Mild, Moderate, Severe, Proliferative DR.

Table 2. Tabulation of different classes using sample images

S. No	Classes	Sample Images
1.	No DR	
2.	Mild	
3.	Moderate	
4.	Severe	
5.	Proliferative DR	

4.2 Experimental Settings

The experiment in this proposed method was performed and validated on a PC with an Intel Core I7-6700 CPU and a working frequency of 3.40 GHz.

Initially, MATLAB realizes both the preprocessing and the retinal image sample set construction. This experiment uses the proposed method to design the network model. This method is trained and tested on the diabetic retinopathy arranged dataset, which contains 35126 images; fundus cameras take all images with distinct image sizes.

4.3 Results Analysis and Discussion

4.3.1 Peak Signal to Noise Ratio (PSNR)

In order to estimate the DR detection performance of the proposed method on different types of lesions in retinal images (i.e., No, DR, mild, moderate, severe, proliferative DR), PSNR, diabetic retinopathy identification accuracy, diabetic retinopathy identification time, sensitivity, specificity are used in this paper to quantify the detection performance of five distinct class labels.

The PSNR is defined as the process of image preprocessing to establish image quality based on the difference between an original image and a denoised image. The difference between the original image size and the preprocessed image size is defined as the mean square error. The PSNR is measured as the ratio between the maximum possible pixel value and the power of noise that affects the quality of the image. The PSNR method is formulated as,

$$PSNR = 10 * \log_{10} \left[\frac{M^2}{Err} \right] \quad (21)$$

$$Err = [S_p - S_o]^2 \quad (22)$$

From the above Equations (21), and (22), the peak signal-to-noise ratio ‘PSNR’ is obtained by taking into consideration the original image ‘S_o’ and preprocessed image ‘S_p’ sizes respectively. PSNR’ is measured in decibels (dB).

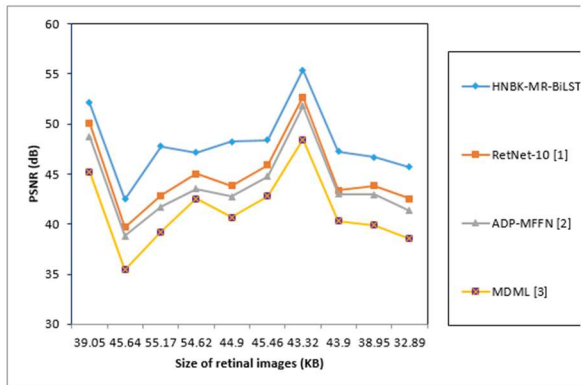


Figure 5: PSNR Versus Size Of Retinal Images

Figure 5 describes the graphical representation of PSNR using the proposed HNBK-MR-BiLSTM method and three state-of-the-art methods [1], [2], and [3]. From the above figure, with distinct sizes of retinal images involved in the procedure for validating diabetic retinopathy, the PSNR rate also varied. However, the comparative analysis describes the improvement in PSNR when applied using existing [1], [2] and [3]. This is inferred from the result with an image size of 39.05KB, where the PSNR using the proposed HNBK-MR-BiLSTM method was 52.11dB, 50.09dB using [1], 48.75dB using [2], and 45.22dB using [3], respectively. These simulation results improved the PSNR rate for the proposed HNBK-MR-BiLSTM method compared to the existing methods. The reason behind the improvement was due to the application of the Hessian Frangi Second-order Partial Derivatives-based Preprocessing algorithm. By applying this algorithm, with three distinct channels, i.e., red channel, green channel, and blue channel, present in the retinal fundus images and subjected to preprocessing, the filtered green images were used for further processing. In contrast, the red and blue images were discarded. Following this, the green images were validated using Frangi Second-order Partial Derivative. By applying this derivative function, not only preserved the edges between points of interest in the sample image, but it also improved the noise ratio significantly using the HNBK-MR-BiLSTM method by 7%, 10%, and 17% compared to [1], [2], and [3].

4.3.2 Diabetic Retinopathy Identification Accuracy

The accuracy rate in the process of identifying DR is measured. The higher the accuracy rate, the more protective the method is, and vice versa. It is defined as accurately detected original images total number of input images are defined as the palmprint detection accuracy. The accuracy is measured as

$$Acc_{DRI} = \sum_{i=1}^n \frac{S_{CI}}{S_i} * 100 \quad (23)$$

In the above Equation (23), the accuracy rate ‘Acc_{DRI}’ is determined based on sample retinal images ‘S_i’ and the number of sample images correctly identified ‘S_{CI}’. The accuracy is measured in terms of percentage (%). Table 2 lists the diabetic retinopathy identification accuracy using the four methods.

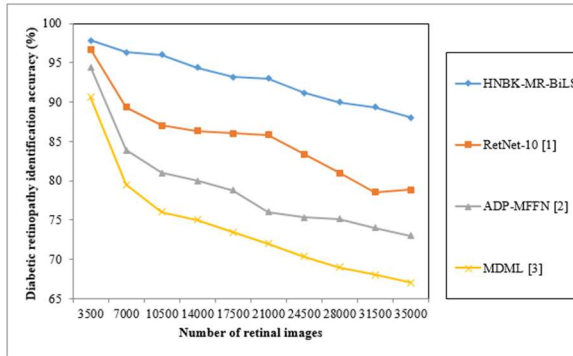


Figure 6: Diabetic Retinopathy Identification Accuracies Versus Numbers Of Retinal Image

Figure 6 represents the graphical representation of diabetic retinopathy identification accuracy with distinct numbers and sizes of fundus images. In the figure, is conditional of diabetic retinopathy identification accuracy is inversely proportional to sample fundus images. In other words, by increasing the number of retinal images, a significant amount of time and error are said to occur, therefore causing a compromise in accuracy. As a result, the overall accuracy of diabetic retinopathy identification is also said to be reduced. However, with simulations performed for 3500 sample retinal images, 3425 sample images were correctly identified using HNBK-MR-BiLSTM, 3385 sample retinal images were correctly identified using [1], 3305 sample retinal images were correctly identified using [2], and 3170 sample retinal images were correctly identified using [3]. With this, the overall diabetic retinopathy identification accuracy was found to be 97.85%, 96.71%, 94.42%, and 90.57% using HNBK-MR-BiLSTM, [1] [2], and [3]. The accuracy rate using HNBK-MR-BiLSTM was mainly improved when compared with [1],[2], and [3]. The accuracy improvement was due to the application of the Bidirectional Multi-scale Retinex LSTM algorithm. By applying this algorithm, both the single-scale retinex function and the multi-scale retinex function were applied to the key points detected. Also, applying the optimized activation function results in the accurate detection of diabetic retinopathy using the HNBK-MR-BiLSTM method by 9%, 18%, and 26% compared to [1], [2], and [3], respectively.

4.3.3 Diabetic Retinopathy Identification Time

In this section, the time consumed in identifying diabetic retinopathy is validated. An amount of time is consumed by identifying diabetic retinopathy. This diabetic retinopathy identification time is measured as given below.

$$T_{DRI} = \sum_{i=1}^n S_i * T(ISI) \quad (24)$$

In the above equation (24), the time factor ‘ T_{DRI} ’ is measured based on sample simulation images ‘ S_i ’ and time consumed in detecting the disease for a single image ‘ $T(ISI)$ ’. Time is measured in milliseconds (ms).

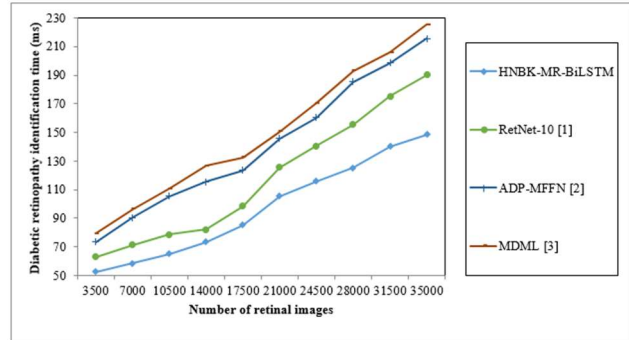


Figure 7: Diabetic Retinopathy Identification Time Versus Number Of Retinal Images

Figure 7 describes the graphical representation of diabetic retinopathy identification time using four different methods. The X-axis is the number of retinal images, and the y-axis is diabetic retinopathy identification time; improving the number of retinal images subsequently increases in diabetic retinopathy identification time. The reason behind the increase is that increasing the frequency of retinal images results in a proportionate amount of noise, and the increase in noise subsequently increases the diabetic retinopathy identification time. However, experimental results are performed in 3500 retinal images, observed 52.5ms of diabetic retinopathy identification time using HNBK-MR-BiLSTM, 63ms of diabetic retinopathy identification time using [1], 73.5ms diabetic retinopathy identification time using [2], and 79.45ms diabetic retinopathy identification time using [3], respectively. The reason for the lesser time consumed in detecting diabetic retinopathy was the application of the Hessian Frangi Second-order Partial Derivatives-based Preprocessing algorithm. The sample input images were initially filtered using the Frangi filter function in the algorithm. This filter function was only applied to the green channel because the green channel included significant information and aided the physicians in denoting different types of fundus image lesions. Hence, the computation time or the diabetic retinopathy identification time was reduced using HNBK-MR-BiLSTM by 17%, 32%, and 36% compared to [1], [2], and [3].

4.3.4 Sensitivity and Specificity

Finally, the sensitivity and specificity rates to correctly identify patients with the presence/absence of disease are validated. This is mathematically formulated as given below.

$$\text{Sensitivity} = \frac{TP}{TP+FN} \quad (25)$$

$$\text{Specificity} = \frac{TN}{TN+FP} \quad (26)$$

From Equations (25) and (26) above, 'TP' is a true positive (i.e., the number of correctly predicted positive samples), 'TN' is true negative (i.e., the number of correctly predicted negative samples), 'FP' is a false positive and finally 'FN' denotes the false negative, respectively.

Table 3 shows the sensitivity and specificity rates with respect to 35000 numbers of retinal images. To be more specific, increasing the number of retinal images causes a proportionate decrease in the sensitivity and specificity rates. However, simulations performed with 3500 retina images saw a sensitivity rate of 0.98 using the HNBK-MR-BiLSTM method, 0.96 using [1], 0.95 using [2], and 0.92 using [3]. Similarly, the simulations performed with 3500 retinal images saw a specificity rate of 0.97 using HNBK-MR-BiLSTM, 0.96 using [1], 0.95 using [2], and 0.91 using [3], respectively. The reason behind the improvement in both the sensitivity and specificity rate was owing to the application of Niblack's Binarization Keypoint Nonlinear Feature Extraction algorithm. By applying this algorithm, the keypoints in a vascular structure that is dark, whereas the optic disc that is bright, as in the green color component, are initially identified.

To identify these keypoints, Niblack's function was applied to obtain the threshold. Following this, the pixel image maps were subjected to high mean and low mean binarization, and orientation measures were also exploited to detect keypoints even in the shift in resolution and orientation. Due to this, the sensitivity rate using the HNBK-MR-BiLSTM method was said to be improved by 3% upon comparison with [1], 5% upon comparison with [2], and 9% upon comparison with [3]. As a result, the specificity rate using the HNBK-MR-BiLSTM method was improved by 4%, 9%, and 13% when compared to [1] [2] [3].

4.4 Ablation Experiments on Feature Selection

In our work, we have used feature selection to eliminate the immaterial or noisy features. The HNBK-MR-BiLSTM technique consists of different feature selection results, namely, relevant and irrelevant features. In this section, ablation studies are performed.

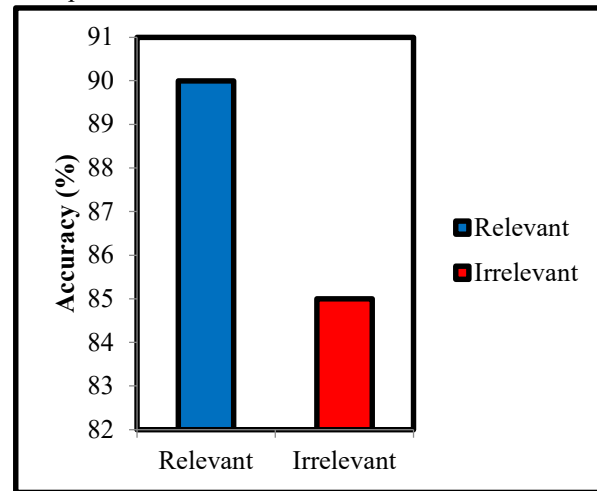


Figure 8: Accuracy Vs Feature Relevance

Figure 8 shows the ablation experiment result for graph feature selection. In the above figure, the x-axis refers to the relevant and irrelevant features, and the y-axis gives the accuracy in percentage (%) for the proposed technique.

4.5 Statistical Test

The analysis of Variance (ANOVA) test is used to analyze the results. It is a type of hypothesis testing that is applied to determine the dissimilarity among the means of two or more groups. The ANOVA test is employed to observe the effects of two independent variables on a dependent variable. Table 4 describes the Statistical analysis using ANOVA test for proposed HNBK-MR-BiLSTM technique with the existing RetNet-10 [1], ADP-MFFN [2], and MDLM [3] using a diabetic retinopathy arranged dataset based on various parameters, such as PSNR, Diabetic Retinopathy Identification Accuracy, Diabetic Retinopathy Identification Time, Sensitivity, and Specificity.

Table 4 Tabulation Of Statistical Analysis Of Proposed HNBK-MR-Bilstm Technique, Existing Retnet-10 [1], ADP-MFFN [2], And MDLM [3] Methods Using ANOVA Test

Methods/Metrics	Two-way ANOVA test			
	HNBK-MR-BiLSTM	RetNet-10 [1]	ADP-MFFN [2]	MDLM [3]
PSNR	48.24	43.83	42.73	40.68
Diabetic Retinopathy Identification Accuracy	93.15	86	78.75	73.45
Diabetic Retinopathy Identification Time	85.15	93.85	123.55	132.65
Sensitivity	0.93	0.91	0.89	0.86
Specificity	0.9	0.86	0.83	0.81

Table 4 demonstrates the overall performance results of different metrics such as PSNR, Diabetic Retinopathy Identification Accuracy, Diabetic Retinopathy Identification Time, Sensitivity, and Specificity for five methods. These results represent that the performance of different parameter using proposed HNBK-MR-BiLSTM technique is significantly improved by 48.24%, 93.15%, 85.15ms, 0.93%, 0.9% which are comparatively higher than the existing methods.

4.6 Discussion

This study compares the proposed HNBK-MR-BiLSTM technique with the existing RetNet-10 [1], ADP-MFFN [2], and MDLM [3] using a diabetic retinopathy arranged dataset based on various parameters, such as PSNR, Diabetic Retinopathy Identification Accuracy, Diabetic Retinopathy Identification Time, Sensitivity, and Specificity are obtained. The results show that the proposed HNBK-MR-BiLSTM method for diabetic retinopathy learns efficiently and improves the classification performance of diabetic retina. The performance analysis of the proposed method to achieve better accuracy, time, sensitivity, specificity, and PSNR compared to different existing methods. The experimental results are achieved by 11%, 18%, 6%, and 8% of improved PSNR, accuracy, sensitivity, and specificity with 28% of minimum time when

compared to the existing [1], [2], [3] using a diabetic retinopathy arranged dataset.

The proposed method exhibits better performance in terms of PSNR, accuracy (97.85%), sensitivity (0.98), specificity (0.97), and low inference time as compared to recent ones [1], [2], [3], [13], and [14]. It has made several distinct advances such as the Hessian Frangi preprocessing, Niblack keypoint extraction, Retinex refinement, and BiLSTM training, which allow achieving more accurate micro-lesion detections, explainability, and robust multi-grade DR classification.

Even though HNBK-MR-BiLSTM demonstrates a high rate of performance, the weaknesses comprise one-dataset testing, the possibility of overfitting because of the complexity of the model, the absence of external validation, and time-sensitiveness. The selected measures are clinically and methodologically sound: PSNR to preprocessing quality, accuracy to general reliability, sensitivity and specificity to diagnostic safety, inference time to real-time viability, and ANOVA to statistical insignificance of the performance improvement.

The proposed method exhibits better performance in terms of PSNR, accuracy (97.85%), sensitivity (0.98), specificity (0.97), and low inference time as compared to recent ones [1], [2], [3], [13], and [14]. It has made several distinct advances such as the Hessian Frangi preprocessing, Niblack keypoint extraction, Retinex refinement, and BiLSTM training, which allow achieving more accurate micro-lesion detections, explainability, and robust multi-grade DR classification.

Even though HNBK-MR-BiLSTM demonstrates a high rate of performance, the weaknesses comprise one-dataset testing, the possibility of overfitting because of the complexity of the model, the absence of external validation, and time-sensitiveness. The selected measures are clinically and methodologically sound: PSNR to preprocessing quality, accuracy to general reliability, sensitivity and specificity to diagnostic safety, inference time to real-time viability, and ANOVA to statistical insignificance of the performance improvement.

5. CONCLUSION AND FUTURE SCOPE

Enormous patients suffering from diabetes and the occurrence of diabetic retinopathy in the midst of them have fostered a great requirement for early diagnosis systems. Over the past few decades, a significant number of research works and a great deal of accomplishments have been made, and satisfactory results have been achieved in several

subdomains. The paper introduces a new and clinically important hybrid architecture of an automated detector of diabetic retinopathy. Through closely combining vessel-conscious preprocessing, nonlinear lesion-related feature construction, and light-insensitive bi-directional learning, the proposed HNBK-MR-BiLSTM model will deliver high-quality diagnostic results in comparison to the current models. The Hessian Frangi Second-order Partial Derivatives-based Preprocessing eliminates the noise in the raw input images. Second, Niblack's Binarization Keypoint Nonlinear Feature Extraction

minimum diabetic retinopathy identification time, enhanced diabetic retinopathy identification accuracy, sensitivity, and specificity. Measured the achieved results using different evaluation metrics, and validation is performed, which outperforms state-of-the-art methods. The information provided in this manuscript is based on the publicly accessed Diabetic Retinopathy Arranged dataset; nevertheless, the pipeline of its methodology, the approach to feature representation, and the structure of the learning are completely new. As compared to earlier studies that directly feed raw images into CNN based classifiers, this paper presents a multi-

can remove more complicated lesion features and improve the overall detection performance with fewer errors and time. In this paper, Niblack's function, low mean binarization, high mean binarization, and optimized activation function are chosen in the feature extraction module, and features are extracted to provide input to the target for classification. Here, a Bidirectional Multi-scale Retinex LSTM classifier is applied to obtain classified results. Extensive experiments are performed to validate the performance of the proposed method in terms of improved PSNR,

step enhancement and representation methodology that explicitly maintains vascular structures, improves micro-lesions and adds illumination correction to classification.

Future research could investigate the incorporation of attention mechanisms and transformer architectures to improve feature extraction in retinal images. Expanding the HNBK-MR-BiLSTM framework to include other ocular conditions and adding real-time mobile diagnostic tools may increase its utility in clinical settings.

Table 3. Tabulation for sensitivity and specificity of proposed HNBK-MR-BiLSTM, RetNet-10 [1], ADP-MFFN [2], and MDLM [3]

Number of retinal images	Sensitivity				Specificity			
	HNBK-MR-BiLSTM	RetNet-10 [1]	ADP-MFFN[2]	MDLM [3]	HNBK-MR-BiLSTM	RetNet-10 [1]	ADP-MFFN [2]	MDLM [3]
3500	0.98	0.96	0.95	0.92	0.97	0.96	0.95	0.91
7000	0.96	0.95	0.93	0.9	0.95	0.93	0.9	0.87
10500	0.95	0.93	0.92	0.89	0.93	0.91	0.88	0.86
14000	0.94	0.92	0.91	0.88	0.91	0.88	0.85	0.83
17500	0.93	0.91	0.89	0.86	0.9	0.86	0.83	0.81
21000	0.92	0.9	0.88	0.85	0.88	0.84	0.8	0.78
24500	0.91	0.88	0.86	0.83	0.86	0.82	0.78	0.75
28000	0.9	0.86	0.85	0.82	0.84	0.8	0.75	0.73
31500	0.89	0.85	0.83	0.8	0.82	0.78	0.72	0.69
35000	0.88	0.83	0.81	0.79	0.8	0.75	0.7	0.66

DECLARATIONS

Conflict of interest: The authors declare that they have no conflict of interest.

Ethical approval: No human or animal studies were conducted by any of the authors for this article.

Funding: There is no funding for this article.

Data availability: The data used to support the findings of this study are publicly available.

Contributions

Formal analysis, Writing, Visualization, Writing – original draft, Alka Singh

Investigation, Resources, Supervision, Conceptualization, Methodology, Writing-review & editing, Rakesh Kumar

Investigation, Resources, Supervision, Conceptualization, Methodology, Writing-review & editing, Amir H Gandomi

REFERENCES

- [1] Mohaimenul, Azam Khan Raiaan, Kaniz Fatema, Inam Ullha Khan, Sami Azam, Md. Rafi Ur Rashid, Md. Saddam Hossain Mukta, Mirjam Jonkman, Friso De Boer, "A Lightweight Robust Deep Learning Model Gained High Accuracy in Classifying a Wide Range of Diabetic Retinopathy Images", IEEE Access, May 2023 [RetNet-10] <https://doi.org/10.1109/ACCESS.2023.3272228>.
- [2] Fangsheng Chen, Shaodong Ma, Jinjui Hao, Mengting Liu, Yuanyan Gu, Quanyong Yi, Jiong Zhang, Yitian Zhao, "Dual-Path and Multi-Scale Enhanced Attention Network for Retinal Diseases Classification Using Ultra-Wide-Field Images", IEEE Access, May 2023 [attention-based dual-path and multi-scale feature fusion network] <https://doi.org/10.1109/ACCESS.2023.3273613>.
- [3] Sharmin Majumder, Nasser Kehtarnavaz, "Multitasking Deep Learning Model for Detection of Five Stages of Diabetic Retinopathy", IEEE Access, Sep 2021 [Multitask deep learning model] <https://doi.org/10.1109/ACCESS.2021.3109240>
- [4] Najib Ullah, Muhammad Ismail Mohmand, Kifaya tUllah, Mohammed S. M. Gismalla, LiaqatAli, Shafqat Ullah Khan, and Niamat Ullah, "Diabetic Retinopathy Detection Using Genetic Algorithm-Based CNN Features and Error Correction Output Code SVM Framework Classification Model", Wireless Communications and Mobile Computing, Wiley, Jul 2022. <https://doi.org/10.1155/2022/7095528>
- [5] Pengxiao Zang, Liqin Gao, Tristan T. Hormel, Jie Wang, Qisheng You, Thomas S. Hwang, and YaliJia, "DcardNet: Diabetic Retinopathy Classification at Multiple Levels Based on Structural and Angiographic Optical Coherence Tomography", Transactions on Biomedical Engineering, Jun 2020. <https://doi.org/10.1109/TBME.2020.3027231>
- [6] Mark A Chia, Fred Hersch, Rory Sayres, Pinal Bavishi, Richa Tiwari, Pearse A Keane, Angus W Turner, "Validation of a deep learning system for the detection, British Journal of Ophthalmology, Feb 2023, <https://doi.org/10.1001/jamaophthalmol.2019.3501>
- [7] Balla Goutam, Mohammad Farukh Hashmi, Zong Woo Geem, Neeraj Dhanraj Bokde, "A Comprehensive Review of Deep Learning Strategies in Retinal Disease Diagnosis Using Fundus Images", IEEE Access, Jun 2022. <https://doi.org/10.1109/ACCESS.2022.3178372>
- [8] Along He, Tao Li, Ning Li, Kai Wang, and Huazhu Fu, "CABNet: Category Attention Block for Imbalanced Diabetic Retinopathy Grading", IEEE Transactions on Medical Imaging, Oct 2017. <https://doi.org/10.1109/TMI.2020.3023463>
- [9] Binhua Yang, Tongyan Li, Haidi Xie, Yulin Liao, Yi-Ping Phoebe Chen, "Classification of Diabetic Retinopathy Severity Based on GCA Attention Mechanism", IEEE Access, Dec 2021
- [10] Wejdan L. Alyoubi, Wafaa M. Shalash, Maysoon F. Abulkhair, "Diabetic retinopathy detection through deep learning techniques: A review", Informatics in Medicine Unlocked, Elsevier, Jun 2020. <https://doi.org/10.1109/ACCESS.2021.3139129>
- [11] Anila Sebastian, Omar Elharrouss, Somaya Al-Maadeed, and Noor Almaadeed, "A Survey on Deep-Learning-Based Diabetic Retinopathy Classification", Diagnostics, Feb 2023 <https://doi.org/10.3390/diagnostics13030345>
- [12] Dolly Das & Saroj Kumar Biswas & Sivaji Bandyopadhyay, "Detection of Diabetic Retinopathy using Convolutional Neural Networks for Feature Extraction and Classification (DRFEC)", Multimedia Tools and Applications, Springer, Oct 2022. <https://doi.org/10.1007/s11042-022-14165-4>
- [13] Mohamed M. Farag, Mariam Fouad, Amr T. Abdel-Hamid, "Automatic Severity Classification of Diabetic Retinopathy Based on DenseNet and Convolutional Block Attention Module", IEEE Access, Apr 2022. <https://doi.org/10.1109/ACCESS.2022.3178372>

2022. <https://doi.org/10.1109/ACCESS.2022.3165193>
- [14] Jingbo Hu, Huan Wang, Le Wang, Ye Lu, "Graph Adversarial Transfer Learning for Diabetic Retinopathy Classification", IEEE Access, Nov 2022. <https://doi.org/10.1109/ACCESS.2022.3220776>
- [15] Chun-Ling Lin and Kun-Chi Wu, "Development of revised ResNet-50 for diabetic retinopathy detection", BMC Bioinformatics, Mar 2023 <https://doi.org/10.1186/s12859-023-05293-1>
- [16] Nurul Mirza Afiqah Tajudin, Kuryati Kipli, Muhammad Hamdi Mahmood, Lik Thai Lim, Dayang Azra Awang Mat, Rohana Sapawi, Siti Kudnie Sahari, Kasumawati Lias, Suriati Khartini Jali, Mohammed Enamul Hoque, "Deep learning in the grading of diabetic retinopathy: A review", IET Computer Vision, Wiley, Jun 2022. <https://doi.org/10.1049/cvi2.12116>
- [17] M. D. Ramasamy, K. Periasamy, L. Krishnasamy, R. K. Dhanaraj, S. Kadry and Y. Nam, "Multi-Disease Classification Model using Strassen's Half of Threshold (SHoT) Training Algorithm in Healthcare Sector," in IEEE Access <https://doi.org/10.1109/ACCESS.2021.3103746>
- [18] Wanghu Chen, Bo Yang, Jing Li, Jianwu Wang, "An Approach to Detecting Diabetic Retinopathy Based on Integrated Shallow Convolutional Neural Networks", IEEE Access, Oct 2020 <https://doi.org/10.1109/ACCESS.2020.3027794>
- [19] Rubina Sarki, Khandakar Ahmed, Hua Wang, Yanchun Zhang, "Automatic Detection of Diabetic Eye Disease Through Deep Learning Using Fundus Images: A Survey", IEEE Access, Aug 2022 <https://doi.org/10.1109/ACCESS.2020.3015258>
- [20] Nikos Tsiknakis, Dimitris Theodoropoulos, Georgios Manikis, Emmanouil Ktistakis, Ourania Boutsora, Alexa Berto, Fabio Scarpa, Alberto Scarpa, Dimitrios I. Fotiadis, Kostas Marias, "Deep learning for diabetic retinopathy detection and classification based on fundus images: A review", Computers in Biology and Medicine, Elsevier, Jun 2021 <https://doi.org/10.1016/j.compbiomed.2021.104599>
- [21] Niloy Sikder, Mehedi Masud, Hesham A. Alhumyani, "Severity classification of diabetic retinopathy using an ensemble learning algorithm through analyzing retinal images", Symmetry. Apr 2021 <https://www.mdpi.com/2073-8994/13/4/670>
- [22] Rêgo, S.; Dutra-Medeiros, M.; Soares, F.; Monteiro-Soares, M. Screening for Diabetic Retinopathy Using an Automated Diagnostic System Based on Deep Learning: Diagnostic Accuracy Assessment. *Ophthalmologica* 2021, 244, 250–257.
- [23] Saha, S.K.; Fernando, B.; Cuadros, J.; Xiao, D.; Kanagasingam, Y. Automated quality assessment of colour fundus images for diabetic retinopathy screening in telemedicine. *J. Digit. Imaging* 2018, 31, 869–878.
- [24] Abbas, Q.; Fondon, I.; Sarmiento, A.; Jiménez, S.; Alemany, P. Automatic recognition of severity level for diagnosis of diabetic retinopathy using deep visual features. *Med. Biol. Eng. Comput.* 2017, 55, 1959–1974.
- [25] Fu, H.; Xu, Y.; Wong, D.W.K.; Liu, J. Retinal vessel segmentation via deep learning network and fully-connected conditional random fields. In Proceedings of the 2016 IEEE 13th International Symposium on Biomedical Imaging (ISBI), Prague, Czech Republic, 13–16 April 2016; pp. 698–701.
- [26] Mo, J.; Zhang, L. Multi-level deep supervised networks for retinal vessel segmentation. *Int. J. Comput. Assist. Radiol. Surg.* 2017, 12, 2181–2193.
- [27] Maji, D.; Santara, A.; Ghosh, S.; Sheet, D.; Mitra, P. Deep neural network and random forest hybrid architecture for learning to detect retinal vessels in fundus images. In Proceedings of the 2015 37th Annual International Conference of the IEEE Engineering in Medicine and Biology Society (EMBC), Milano, Italy, 25–29 August 2015; pp. 3029–3032.
- [28] Maya, K.V.; Adarsh, K.S. Detection of Retinal Lesions Based on Deep Learning for Diabetic Retinopathy. In Proceedings of the 2019 Fifth International Conference on Electrical Energy Systems (ICEES), Chennai, India, 21–22 February 2019; pp. 1–5.

- [29] Raja, C.; Balaji, L. An automatic detection of blood vessel in retinal images using convolution neural network for diabetic retinopathy detection. *Pattern Recognit. Image Anal.* 2019, 29, 533–545.
- [30] Tang, F.; Luenam, P.; Ran, A.R.; Quadeer, A.A.; Raman, R.; Sen, P.; Khan, R.; Giridhar, A.; Haridas, S.; Igllicki, M.; et al. Detection of Diabetic Retinopathy from Ultra-Widefield Scanning Laser Ophthalmoscope Images: A Multicenter Deep Learning Analysis. *Ophthalmol. Retin.* 2021, 5, 1097–1106.
- [31] Hua, C.-H.; Huynh-The, T.; Kim, K.; Yu, S.-Y.; Le-Tien, T.; Park, G.H.; Bang, J.; Khan, W.A.; Bae, S.-H.; Lee, S. Bimodal learning via trilogy of skip-connection deep networks for diabetic retinopathy risk progression identification. *Int. J. Med. Inform.* 2019, 132, 103926.
- [32] Qummar, S.; Khan, F.G.; Shah, S.; Khan, A.; Shamshirband, S.; Rehman, Z.U.; Khan, I.A.; Jadoon, W. A deep learning ensemble approach for diabetic retinopathy detection. *IEEE Access* 2019, 7, 150530–150539.
- [33] Jadhav, A.S.; Patil, P.B.; Biradar, S. Optimal feature selection-based diabetic retinopathy detection using improved rider optimization algorithm enabled with deep learning. *Evol. Intell.* 2020, 14, 1431–1448.
- [34] Hemanth, D.J.; Deperlioglu, O.; Kose, U. An enhanced diabetic retinopathy detection and classification approach using deep convolutional neural network. *Neural Comput. Appl.* 2020, 32, 707–721.
- [35] Adriman, R.; Mughtar, K.; Maulina, N. Performance Evaluation of Binary Classification of Diabetic Retinopathy through Deep Learning Techniques using Texture Feature. *Procedia Comput. Sci.* 2021, 179, 88–94.
- [36] Bhatti, E.; Kaur, P. DRAODM: Diabetic retinopathy analysis through optimized deep learning with multi support vector machine for classification. In *Proceedings of the International Conference on Recent Trends in Image Processing and Pattern Recognition, Solapur, India, 21–22 December 2018*; pp. 174–188.
- [37] Diabetic Retinopathy Arranged dataset: <https://www.kaggle.com/amanneo/diabetic-retinopathy-resized-arranged>.